

Design of Low-Cost Fuzzy Controllers with Reduced Parametric Sensitivity Based on Whale Optimization Algorithm

Radu-Codrut David

*Department of Automation and Applied Informatics
Politehnica University of Timisoara
Timisoara, Romania
davidradu@gmail.com*

Alexandra-Iulia Szedlak-Stinean

*Department of Automation and Applied Informatics
Politehnica University of Timisoara
Timisoara, Romania
alexandra-iulia.stinean@aut.upt.ro*

Radu-Emil Precup

*Department of Automation and Applied Informatics
Politehnica University of Timisoara
Timisoara, Romania
radu.precup@upt.ro*

Raul-Cristian Roman

*Department of Automation and Applied Informatics
Politehnica University of Timisoara
Timisoara, Romania
raul.roman@aut.upt.ro*

Stefan Preitl

*Department of Automation and Applied Informatics
Politehnica University of Timisoara
Timisoara, Romania
stefan.preitl@upt.ro*

Emil M. Petriu

*School of Electrical Engineering and Computer Science.
University of Ottawa
Ottawa, ON, Canada
petriu@uottawa.ca*

Abstract—The aim of this paper is to demonstrate the feasibility of Whale Optimization Algorithm (WOA) in solving complex control design and tuning problems of fuzzy control systems (FCSs) with a reduced parametric sensitivity. The sensitivity analysis of these FCSs implies the use of sensitivity models defined with respect to the parametric variations of the processes. The main goal is solving the optimization problems defined for servo system processes controlled by Takagi-Sugeno-Kang proportional-integral fuzzy controllers (TSK PI-FCs), through minimization of objective functions that include the output sensitivity functions. A design method is proposed in this regard, and it is validated through experimental results using a laboratory nonlinear servo system.

Keywords— experimental validation, fuzzy control system, parametric sensitivity, Whale optimization algorithm

I. INTRODUCTION

The current design of fuzzy controllers (FCs) has taken a steep rise in recent years [1]–[5]. Still, in real life applications, the controlled processes for which fuzzy control systems (FCSs) are designed and tuned are subjected to parametric variations; therefore, a sensitivity analysis with respect to the parametric variations of the controlled process is required. Nevertheless, the optimization of FCs together with sensitivity models is a difficult challenge, mainly because the mathematical models used, employ non-convex and/or non-differentiable objective functions (OFs). The minimization of these OFs with the aid of Whale Optimization Algorithm (WOA) expresses this papers' main objective, formulated in the framework of an optimization problem (OP). A second objective is the introduction of a WOA-based design method for the optimal tuning of Takagi-Sugeno-Kang Proportional-Integral fuzzy controllers (TSK PI-FCs) with a reduced process parametric sensitivity.

In solving this type of OPs, various nature-inspired optimization algorithms (NIOAs) can be employed with a significant success rate. Particle Swarm Optimization (PSO) is employed in [6] to identify fuzzy parameters in a zero-order Takagi-Sugeno system with a standard fuzzy partition. Gravitation Search Algorithm (GSA) is employed

in [7] for the optimization of a Takagi-Sugeno fuzzy model using in wind power interval prediction. A hybrid Firefly-PSO is introduced in [8] for optimizing the parameters of an interval type-2 fractional order fuzzy proportional integral derivative based power system stabilizer with the aim of minimizing low-frequency oscillations in a power system. Proportional-Integral-Derivative (PID) and Proportional-Integral (PI) fuzzy control in interconnected hydro-thermal power system, servo systems and tower crane systems is based on Grey Wolf Optimizer (GWO) in [9]–[13].

The third objective set for this paper is the development of a reduced sensitivity solution for TSK PI-FCs with respect to a small time constant of the process. In order to achieve this objective, a sensitivity analysis with respect to the variations of that parameter will be conducted. Deriving the obtained sensitivity models is required prior to their addition to the OFs. Solving the OP associated to the combined mathematical models, requires the use of a substantial level of computational resources; therefore, a WOA-based solution is desired in order to avoid this downside.

WOA [14] is a newly introduced method in the variety of NIOAs which is getting good traction [15]–[17]. WOA bases its mathematical model on the social behavior and interaction of humpback whales. WOA uses three operators to simulate the phases of the hunting behavior namely: search for prey, encircling prey and bubble-net foraging. As presented in [14], WOA has a competitive performance compared to other well-known NIOAs. In [15] a modified WOA is used for tuning the parameter of an adaptive fuzzy logic PID controller used for load frequency control of an autonomous power generation system. Similarly, in [16] the controller parameters of a fuzzy lead-lag controller employed in a coordinated structure combining static synchronous series compensator and power system stabilizer are tuned using a WOA derived for balancing exploration and exploitation stages. An upgraded WOA is introduced in [17] for parameter tuning of an FC applied to a seismically excited nonlinear steel building. All these applications are relying on variants of WOA designed for specific OPs. Although the results have shown

improvements compared to the standard version of WOA, they lose the ease of implementation for WOA, as each case would require a specific version. As stated, the main goal is to use the standard version of WOA in solving our OP.

The following sections of this paper will be structured as follows: in Section II the optimization problem is defined for the FCS and associated models are given, Section III is dedicated to the novel solution to the OP based on WOA, which produces optimally tuned TSK PI-FCs, focused on servo system processes modeled by second-order dynamics with an integral component, and the design method is formulated, experimental results and a case study for WOA-solution is included in Section IV, while Section V presents the conclusions.

II. OPTIMIZATION PROBLEM AND MODELS

The FCS structure is given in Fig. 1, where C is the fuzzy controller, P is the nonlinear process, F is the set-point filter, r is the set-point (the reference input), r_1 is the filtered reference input, y is the controlled output, u is the control signal, and $e = r_1 - y$ is the control error. Disturbance inputs are not considered in Fig. 1 because the integral component in the controller ensures the disturbance rejection.

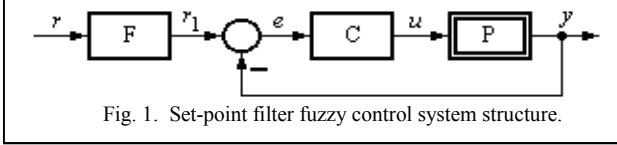


Fig. 1. Set-point filter fuzzy control system structure.

Fig. 1 illustrates a set-point filter control system (CS) structure in the framework of two-degree-of-freedom (2-DOF) CS structures. The parameters of both F and C blocks can be tuned.

The state-space model of P specific to the nonlinear servo systems is

$$n_{sdz}(t) = \begin{cases} -1, & \text{if } u(t) \leq -u_b, \\ [u(t) + u_c]/(u_b - u_c), & \text{if } -u_b < u(t) < -u_c, \\ 0, & \text{if } -u_c \leq |u(t)| \leq u_a, \\ [u(t) - u_a]/(u_b - u_a), & \text{if } u_a < u(t) < u_b, \\ 1, & \text{if } u(t) \geq u_b, \end{cases}$$

$$\begin{bmatrix} \dot{x}_1(t) \\ \dot{x}_2(t) \end{bmatrix} = \begin{bmatrix} 0 & 1 \\ 0 & -1/T_\Sigma \end{bmatrix} \begin{bmatrix} x_1(t) \\ x_2(t) \end{bmatrix} + \begin{bmatrix} k_p \\ T_\Sigma \end{bmatrix} n_{sdz}(t),$$

$$y(t) = [1 \ 0] [x_1(t) \ x_2(t)]^T, \quad (1)$$

where $t \geq 0$ is the continuous time, $k_p > 0$ is the process gain, $T_\Sigma > 0$ is the small time constant, the control signal $u(t)$ applied to the DC motor is a pulse width modulated duty cycle, $x_1(t) = \alpha(t)$ is the angular position, $x_2(t) = \omega(t)$ is the angular speed, and the superscript T indicates matrix transposition. The variable $n_{sdz}(t)$ is the output of the saturation and dead zone static nonlinearity, which is modeled by the first equation in (1) with the parameters u_a , u_b and u_c , $0 < u_a < u_b$, $0 < u_c < u_b$.

The state-space model (1) includes the actuator and measurement instrumentation dynamics. The nonlinearity in (1) is not symmetric, and this offers a more general model compared to that investigated in [18].

The nonlinearity in (1) is neglected in the simplified model of the process expressed as the transfer function (t.f.) $P(s)$

$$P(s) = k_{EP}/[s(1 + T_\Sigma s)], \quad (2)$$

where k_{EP} is the equivalent process gain

$$k_{EP} = \begin{cases} k_p/(u_b - u_c), & \text{if } -u_b < u(t) < -u_c, \\ k_p/(u_b - u_a), & \text{if } -u_a < u(t) < -u_b. \end{cases} \quad (3)$$

It is convenient to use $P(s)$ in the linear and fuzzy controller design and tuning in two cases out of the five cases concerning the nonlinearity in (1). As shown in [19], PI controllers can cope with the process modeled in (2) in terms of Fig. 1, with a PI controller instead of FC. The PI controller t.f. is

$$C(s) = k_c/(1 + sT_i)/s = k_c[1 + 1/(sT_i)], \quad k_c = k_c T_i \quad (4)$$

where $k_c > 0$ (or $k_c > 0$) is the controller gain and $T_i > 0$ is the integral time constant.

Considering that the process parameters k_p and T_Σ are variable and the other ones are constant, the process parameter vector is

$$\alpha = [\alpha_1 \ \alpha_2]^T = [k_p \ T_\Sigma]^T \quad (5)$$

The definitions of the state sensitivity functions $\lambda_v, v = 1..n$, and output sensitivity function σ are

$$\lambda_v = \left[\frac{\partial x_v}{\partial \alpha_\tau} \right]_0, \quad \sigma = \left[\frac{\partial y}{\partial \alpha_\tau} \right]_0, \quad v = 1..n, \tau \in \{1,2\}, \quad (6)$$

where the subscript 0 indicates the nominal value of the process parameter $\alpha_j, j \in \{1,2\}$, and n is the number of state variables of the FCS. The state sensitivity models of the FCS with respect to α_j are derived using (6), with $n = 4$ for TSK-PI-FCs.

Using the notation ρ for the controller parameter vector, $\rho \in R^m$, the OP that ensures the sensitivity reduction with respect to the modifications of the process parameter α_j is defined as

$$\rho^* = \arg \min_{\rho \in D_\rho} J(\rho),$$

$$J(\rho) = \sum_{d=0}^{\infty} \{e^2(t_d, \rho) + \gamma^2[\sigma(t_d, \rho)]^2\}, \quad (7)$$

where γ is a customizable weighting parameter, ρ^* is the optimal controller parameter vector (the optimal value of ρ), D_ρ is the feasible domain of ρ , $D_\rho \subset R^m$, $J(\rho)$ is the OF, and $t_d \in Z, t_d \geq 0$, is the discrete time argument.

The ESO method [19] is applied to tune the PI controller parameters in (4), and it guarantees a trade-off to the linear CS performance specifications (maximum values of CS performance indices, i.e., percent overshoot, settling time and rise time) of the linear CS using only one design parameter β within the largest recommended domain $1 < \beta \leq 20$. The PI tuning conditions specific to the ESO method are

$$k_c = 1/(\beta \sqrt{\beta} k_{EP} T_\Sigma^2), \quad T_i = \beta T_\Sigma, \quad k_C = 1/(\sqrt{\beta} k_{EP} T_\Sigma) \quad (8)$$

and the t.f. of F that exhibits CS performance improvement by the cancellation of a closed-loop CS zero is

$$F(s) = 1/(1 + \beta T_\Sigma s). \quad (9)$$

The TSK PI-FCs are designed and tuned using the knowledge from the PI controller structure to ensure an additional CS performance improvement. The structure and the input membership functions of a cost-effective TSK PI-FC are presented in Fig. 2, where q^{-1} is the backward shift operator, TISO-FC is the Two Inputs-Single Output fuzzy controller block that produces a nonlinear input-output static map, $\Delta e(t_d)$ is the increment of control error, and $\Delta u(t_d)$ is the increment of control signal.

The two increments result by discretizing the continuous-time PI controller by Tustin's method, which leads to the recurrent equation of the incremental discrete-time PI controller

$$\Delta u(t_d) = K_p [\Delta e(t_d) + \mu e(t_d)] \quad (10)$$

and its parameters K_p and μ

$$K_p = k_c(T_i - T_S/2), \quad \mu = 2T_S/(2T_i - T_S) \quad (11)$$

where $T_S > 0$ is the sampling period.

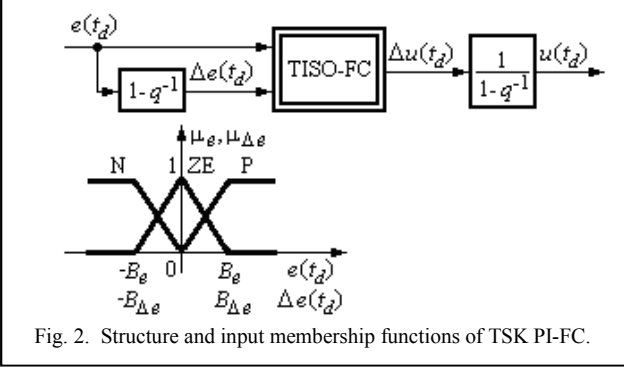


Fig. 2. Structure and input membership functions of TSK PI-FC.

As shown in [20], TISO-FC employs the weighted average method for defuzzification, and the SUM and PROD operators in the inference engine. The rule base is
IF ($e(t_d)$ IS N AND $\Delta e(t_d)$ IS N)
OR ($e(t_d)$ IS P AND $\Delta e(t_d)$ IS P)
THEN $\Delta u(t_d) = \eta K_p [\Delta e(t_d) + \mu e(t_d)]$,
IF ($e(t_d)$ IS ZE) OR ($e(t_d)$ IS N AND $\Delta e(t_d)$ IS ZE)
OR ($e(t_d)$ IS N AND $\Delta e(t_d)$ IS P)
OR ($e(t_d)$ IS P AND $\Delta e(t_d)$ IS ZE)
OR ($e(t_d)$ IS P AND $\Delta e(t_d)$ IS P)
THEN $\Delta u(t_d) = K_p [\Delta e(t_d) + \mu e(t_d)]$ (12)

The parameter η , with the largest domain $0 < \eta < 1$, is introduced to mitigate the fuzzy CS overshoot, which occurs if the two TISO-FC inputs have the same signs. This controller structure and the rule base given in (12) indicate that our cost-effective TSK PI-FC behaves as a bump-less interpolator between two linear PI controllers.

The modal equivalence principle [21] is applied to this TSK PI-FC resulting in the tuning equation

$$B_{\Delta e} = \mu B_e = 2T_s B_e / (2\beta T_\Sigma - T_s) \quad (13)$$

which along with (8), (10) and (11) give the parameter vector of TSK PI-FC

$$\boldsymbol{\rho} = [\beta \ B_e \ \eta]^T \quad (14)$$

with $m = 3$ in order to match the OP in (7).

The parameter vector expressed in (14), associated to the OP defined in (7), will be obtained in the next section by the WOA-based tuning approach.

Accepting that u is changing at the discrete sampling intervals and the presence of the zero-order hold, the derivation of the output sensitivity function $\sigma(t_d)$ requires the state sensitivity model of the fuzzy CS. With this regard the state variables x_3 and x_4 of the TSK PI-FC are defined in terms of [18]

$$x_3(t_d) = u(t_d - 1), \quad x_4(t_d) = e(t_d - 1) \quad (15)$$

and the state variable of F, x_5 , is its output.

For a constant FCS input, namely $r(t) = \text{const}$, assuming $r_1(t) = \text{const}$ for simplicity, the discrete-time state sensitivity model of the FCS with respect to T_Σ is obtained by applying (6) to the discrete-time state-space model of the FCS with the state variables x_1, x_2, \dots, x_5 . The nonlinear input-output static map of TISO-FC is involved in the expression of $\sigma(t_d)$. The expression of the state sensitivity model of FCS is given in [22].

III. WHALE OPTIMIZATION ALGORITHM-BASED SOLUTION INTEGRATION AND FUZZY CONTROLLER DESIGN METHOD

The operation principle of WOA is comprised on three separate stages [14]: encircling the prey, spiral bubble-net feeding maneuver, and search for prey. The location of the agents employed in WOA is described using a position vector $\boldsymbol{x}_i \in R^m$:

$$\boldsymbol{x}_i = [x_i^1 \ \dots \ x_i^j \ \dots \ x_i^m]^T, \quad i = 1 \dots N, \quad (16)$$

where x_i^j is the position of i^{th} agent in j^{th} dimension, $j = 1 \dots m$, and N is the number of agents in the population.

The ability of humpback whales to recognize the location of the prey and encircle them is modeled in the WOA. Based on the fact that the position of the optimal agent is not known a priori in the search space, WOA assumes, as most NIOAs, that the best candidate position is the target or is close enough to the optimum position.

For modeling the prey encircling method at each iteration k , a set of search coefficient vectors $\boldsymbol{a}_i(k) \in R^m$ and $\boldsymbol{c}_i(k) \in R^m$ are introduced:

$$\boldsymbol{a}_i(k) = [a_i^1(k) \ \dots \ a_i^j(k) \ \dots \ a_i^m(k)]^T, \quad (17)$$

$$\boldsymbol{c}_i(k) = [c_i^1(k) \ \dots \ c_i^j(k) \ \dots \ c_i^m(k)]^T, \quad (18)$$

with elements defined as:

$$a_i^j(k) = a(k)(2r^j - 1) \quad (19)$$

$$a(k) = 2[1 - (k - 1)/(k_{\max} - 1)] \quad (20)$$

$$c_i^j(k) = 2r^j \quad (21)$$

where $i = 1 \dots N$, r^j are uniformly distributed numbers within $0 \leq r^j \leq 1$, $j = 1 \dots m$, the scalar coefficients $a^j(k)$ are linearly decreased from 2 to 0 for all stages of the search process including exploration and exploitation. k is the iteration index in WOA, $k = 1 \dots k_{\max}$, and k_{\max} is the maximum number of iterations.

The mathematical model of the next phase, bubble-net attacking method, is associated to the exploitation phase of WOA and is comprised of two approaches: shrinking encircling and spiral position updating. The shrinking encircling mechanism model is attained by decreasing the value of $a(k)$ in terms of (20), which determines the range variation of $a_i^j(k)$ to $[-a(k), a(k)]$.

The first step in the spiral position updating calculates the distance vector $\boldsymbol{d}_i(k)$ of i^{th} agent between the current agent vector $\boldsymbol{x}_i(k)$ and the best agents' position (prey) vector $\boldsymbol{x}_{best}(k)$ in the population at the iteration k .

$$\boldsymbol{x}_{best}(k) = [x_{best}^1(k) \ \dots \ x_{best}^j(k) \ \dots \ x_{best}^m(k)]^T \in R^m \quad (22)$$

Using the notation J for the OF, $\boldsymbol{x}_{best}(k)$ is computed in terms of

$$J(\boldsymbol{x}_{best}(k)) = \min_{i=1 \dots N} \{J(\boldsymbol{x}_i(k))\} \quad (23)$$

which also indicates that

$$J(\boldsymbol{x}_{best}(k)) \leq J(\boldsymbol{x}_i(k)), \quad i = 1 \dots N. \quad (24)$$

The general expression of the distance vector $\boldsymbol{d}_i(k)$ of i^{th} agent at iteration k is

$$\boldsymbol{d}_i(k) = [d_i^1(k) \ \dots \ d_i^j(k) \ \dots \ d_i^m(k)]^T \in R^m \quad (25)$$

and its elements, which depend on the elements of $\boldsymbol{x}_i(k)$ (defined in (16)) and $\boldsymbol{x}_{best}(k)$ (defined in (22)), are obtained as

$$d_i^j(k) = |x_i^j(k) - x_{best}^j(k)|, \quad j = 1 \dots m, \quad i = 1 \dots N. \quad (26)$$

The helix shaped movement of the agent is modeled using a spiral equation using the current agents' position and the best solution:

$$\boldsymbol{x}_i(k+1) = \boldsymbol{d}_i(k)e^{bl} \cos(2\pi l) + \boldsymbol{x}_{best}(k), \quad (27)$$

where $b = \text{const}$ is used to define the shape of the logarithmic spiral, set to $b = 1$ for simplifying the shape, and l is a uniformly distributed number, $-1 \leq l \leq 1$.

As the humpback whales swim around the prey within a shrinking circle and along a spiral-shaped path simultaneously, a probability-based model is introduced using a 50% chance to choose from either position update methods. The position update in (27) is further modified

$$\boldsymbol{x}_i(k+1) = \begin{cases} \boldsymbol{d}_i(k)e^{bl} \cos(2\pi l) + \boldsymbol{x}_{best}(k) & \text{if } p \geq 0.5 \\ \boldsymbol{x}_{best}(k) - \boldsymbol{f}_i(k) & \text{otherwise} \end{cases} \quad (28)$$

where p is random number, $0 \leq p \leq 1$, and the vector $\mathbf{f}_i(k)$ is computed as

$$\begin{aligned}\mathbf{f}_i(k) &= [f_i^1(k) \dots f_i^j(k) \dots f_i^m(k)]^T \\ &= [a_i^1(k)d_i^1(k) \dots a_i^j(k)d_i^j(k) \dots a_i^m(k)d_i^m(k)]^T \in R^m\end{aligned}\quad (29)$$

Our WOA implementation will make further use of the update equation (28) instead of (27). A further addition with the goal of extending the exploration capabilities, even in later stages of the search process, is introduced when $p < 0.5$ and $|a_i^j(k)| > 1$. This extension introduces an arbitrary component in order to force the agents to move from a reference point by choosing a random agents' position instead of the global solution.

For this case $\mathbf{g}_i(k)$ is defined as:

$$\begin{aligned}\mathbf{g}_i(k) &= [g_i^1(k) \dots g_i^j(k) \dots g_i^m(k)]^T \\ &= [a_i^1(k)g_i^1(k) \dots a_i^j(k)g_i^j(k) \dots a_i^m(k)g_i^m(k)]^T \in R^m\end{aligned}\quad (30)$$

Thus, the elements are calculated as:

$$g_i^j(k) = |x_i^j(k) - x_{rand}^j(k)|, j = 1 \dots m, i = 1 \dots N \quad (31)$$

where $rand$ is the arbitrary agent index.

Summing up, the complete position update model becomes

$$\begin{cases} \mathbf{x}_i(k+1) = \\ \begin{aligned} &\mathbf{x}_{best}(k) - \mathbf{f}_i(k), \\ &\text{if } p < 0.5 \text{ and } |a_i^j(k)| \leq 1, \forall j = 1 \dots m \\ &\mathbf{x}_{rand}(k) - \mathbf{g}_i(k), \\ &\text{if } p < 0.5 \text{ and } |a_i^j(k)| > 1, \forall j = 1 \dots m \\ &\mathbf{d}_i(k)e^{bl} \cos(2\pi l) + \mathbf{x}_{best}(k), \\ &\text{otherwise} \end{aligned} \end{cases} \quad (32)$$

Equation (32) is repeated by incrementing the iteration index k until k_{max} is reached. The initial whale population, represented by N agents' positions in the m -dimensional search space, is generated randomly using the a priori information on the OP.

Equations (16), (23) and (32) are used for the integration of the WOA onto the OP defined in (7) as follows:

$$\boldsymbol{\rho} = \mathbf{x}_i(k), i = 1 \dots N, \quad (33)$$

$$\boldsymbol{\rho}^* = \arg \min_{i=1 \dots N} J(\mathbf{x}_i(k_{max})). \quad (34)$$

Equation (34) indicates that WOA is stopped at iteration k_{max} , and the final solution obtained so far is actually the solution to the OP defined in (7). Therefore, the formation of the design method for TSK PI-FCs is completed.

Based on the aspects presented in the previous and current sections, the design method dedicated to TSK PI-FCs is described by the following design steps:

Step 1. The sampling period is set in accordance with the requirements of quasi-continuous digital control, and the sensitivity model of the FCS is derived.

Step 2. The weighting parameter γ in (7) is set with the aim of meeting the performance specifications of FCS. The values of γ were considered such that the ratio of the two right-hand members in (7) to take the values $\{0, 0.1, 1, 10\}$.

As well, in this step, the feasible domain $D_{\boldsymbol{\rho}}$ is set to include all constraints imposed to the elements of $\boldsymbol{\rho}$. For example, inequalities resulted from the stability analysis of FCS can be included to define $D_{\boldsymbol{\rho}}$. Several representative constraints including stability ones can be applied from [23]–[30] by adapting them to this FCS structure.

Step 3. WOA is integrated in solving the OP in (7) thus resulting the optimal value of the parameter vector $\boldsymbol{\rho}^*$ and the optimal parameters β^*, B_e^*, η^* (for $m = 3$):

$$\begin{aligned}\boldsymbol{\rho}^* &= [\rho_1^* \quad \rho_2^* \quad \rho_3^*], \\ \rho_1^* &= \beta^*, \rho_2^* = B_e^*, \rho_3^* = \eta^*.\end{aligned}\quad (35)$$

Step 4. The optimal value of the parameter $B_{\Delta e}^*$ of TSK PI-FC results from the expression of (13) calculated for the optimal parameter values from (35).

$$B_{\Delta e}^* = 2T_s B_e^*/(2\beta^* T_\Sigma - T_s). \quad (36)$$

The t.f. of F is obtained from the following expression of (9) for $\beta = \beta^*$:

$$F(s) = 1/(1 + \beta^* T_\Sigma s). \quad (37)$$

The nominal value of T_Σ is thus employed in the design of TSK PI-FCs as shown by (36) and (37).

IV. EXPERIMENTAL VALIDATION

The proposed optimization method that optimally tunes the parameters TSK PI-FCs is validated using the INTECO DC servo system laboratory equipment. The main features of the experimental setup are [31]: rated amplitude of 24 V, rated current of 3.1 A, rated torque of 15 N cm, rated speed of 30000 rpm, and weight of inertial load of 2.03 kg.

The parameters of the linear dynamics of the process models presented in (1) and (2) have the following values: $u_a = 0.15$, $u_b = 1$, $u_c = 0.15$, $k_{P0} = k_{EP0} = 140$ and $T_{\Sigma 0} = 0.92$ s. Since a reduced process small time constant sensitivity is targeted, T_Σ is variable, therefore $\alpha_1 = T_\Sigma$ in (6).

Steps 1 to 4 given in the previous section were applied for validating the proposed design method. Step 1 starts with defining the value for the sampling period as $T_s = 0.01$ s in order to fulfill the conditions for quasi-continuous digital control.

The weighting parameter in (7) in step 2 is set such that to take four possible values, $\gamma^2 \in \{0, 0.002214, 0.02214, 0.2214\}$, to satisfy the parameter ratio restriction imposed for this step. The search space representing the feasibility domain of $\boldsymbol{\rho}$ was set to:

$$D_{\boldsymbol{\rho}} = \{3 \leq \beta \leq 17\} \times \{20 \leq B_e \leq 40\} \times \{0.55 \leq \eta \leq 0.75\}. \quad (38)$$

Step 3 deals with the evaluation of the OF $J(\boldsymbol{\rho})$ using an experimental scenario characterized by a time horizon of 20s in terms of the dynamic regimes of the CS with respect to the step-type modification of the reference input r to measure the values of $J(\boldsymbol{\rho})$. The presented results were obtained for the $r = 40rad$ step-type modification of r . The only parameters of WOA used in this step are $N = 20$ and $k_{max} = 100$.

The optimal values of the tuned controller parameters obtained using the WOA-based design method are presented in Table I. The values presented are the best results obtained by using five trials on each scenario.

The results for the weighting parameters and controller parameters obtained using WOA-based design method are compared in Table II with other NIOAs: GWO, GSA and PSO applied in [11], [18] and [22] in the same way in Step 3 instead of WOA. The main parameter values of GWO, GSA and PSO are the same of those for WOA, namely $N = 20$ and $k_{max} = 100$; this ensures a fair comparison. The other search process parameters values specific to GWO, GSA and PSO are specified in [11], [18] and [22].

The data given in Table II demonstrates that our WOA-based solution leads to similar values with marginal improvements in majority of cases. Therefore, the design method proposed here is a viable alternative to solve (7) with a reduced implementation complexity compared to other NIOAs due to the reduced number of parameters.

TABLE I. WEIGHTING PARAMETER AND CONTROLLER PARAMETERS FOR WOA-BASED MINIMIZATION OF J

$(\gamma)^2$	B_e^*	η^*	$B_{\Delta e}^*$	β^*	k_c^*	T_i^*	J
0	40	0.75	0.1385	3.1438	0.0044	2.8923	390459
0.002214	40	0.75	0.1386	3.1421	0.0044	2.8907	393501
0.02214	40	0.75	0.1388	3.1276	0.0044	2.8774	421012
0.2214	40	0.75	0.1366	3.1388	0.0044	2.8811	693374

TABLE II. WEIGHTING PARAMETER AND CONTROLLER PARAMETERS FOR NIOA-BASED MINIMIZATION OF J

	$(\gamma)^2$	B_e^*	η^*	$B_{\Delta e}^*$	β^*	k_c^*	T_i^*	J
GWO	0	40	0.75	0.1386	3.1433	0.0044	2.8919	390459
	0.002214	40	0.75	0.1388	3.1369	0.0043	2.8859	393508
	0.02214	40	0.75	0.1387	3.1395	0.0044	2.8883	421041
	0.2214	40	0.75	0.1332	3.2686	0.0043	3.0071	695761
GSA	0	40	0.75	0.1385	3.1437	0.0044	2.8922	390459
	0.002214	39.9979	0.75	0.1385	3.1454	0.0044	2.8937	393520
	0.02214	40	0.75	0.1393	3.1274	0.0044	2.8772	421083
	0.2214	40	0.75	0.1369	3.1813	0.0043	2.9268	696525
PSO	0	40	0.75	0.1452	3	0.0045	2.76	392076
	0.002214	40	0.75	0.1452	3	0.0045	2.76	395143
	0.02214	40	0.75	0.1395	3.1211	0.0044	2.8714	420966
	0.2214	40	0.75	0.1452	3	0.0045	2.76	698859

The performance of the presented algorithm was quantified using two performance indices. The first index relates to the convergence speed c_s of the WOA algorithm by measuring the number of evaluations required for $J(\rho)$ before the optimal solution ρ^* is reached.

The second performance index evaluates the accuracy of WOA. Before defining it, the average value of the OF $J(\rho)$ is introduced as:

$$Avg(J_{min}) = \left(\frac{1}{N_{best}} \sum_{h=1}^{N_{best}} J_{min}^{(h)} \right) \quad (39)$$

where J_{min} is the value of $J(\rho)$ obtained after using the WOA-based solution, N_{best} is the number of best values used for this index and is set to $N_{best} = 5$ and the superscript h indicates the observed trial, $1 \leq h \leq N_{best}$.

The accuracy rate a_r is defined as the percent of standard deviation of $J(\rho)$ obtained by running WOA divided to $Avg(J_{min})$:

$$a_r = StDev\% (J_{min}) = 100 \frac{StDev(J_{min})}{Avg(J_{min})}$$

$$StDev(J_{min}) = \sqrt{\frac{1}{N_{best}-1} \sum_{h=1}^{N_{best}} (J_{min}^{(h)} - Avg(J_{min}))^2} \quad (40)$$

The values provided in Table III show the search performance of WOA in terms of accuracy and resource usage. In addition, this way of presenting the performance is fair in because it mitigates the effects of the random parameters of WOA on both WOA and FCS performance.

TABLE III. VALUES OF PERFORMANCE INDICES c_s AND a_r

$(\gamma)^2$	c_s	a_r
0	93	0
0.002214	79	0.0016
0.02214	65	0.098
0.2214	94	0.1813

Fig. 3 gives the experimental results that correspond to the FCS with the TSK PI-FC that operates with the parameters given in the second row of Table I and for the nominal process. The average OF measured for FCS is $J = 393519$.

The results show that the nonlinearity of the servo system as the proportional component of the controller is not capable of triggering an aggressive control signal. Consequently, the level of the control signal varies in the vicinity of the dead zone. The time responses of the experimental results were influenced by the friction in the bearings of the experimental setup.

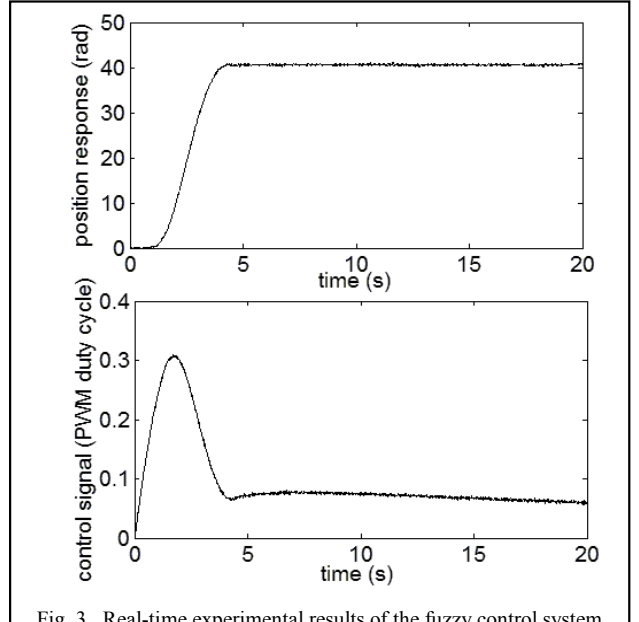


Fig. 3. Real-time experimental results of the fuzzy control system for the nominal process parameters.

V. CONCLUSION

This paper has achieved its main objective of introducing a viable WOA-based solution to the optimal tuning of fuzzy controllers with a reduced process small time constant sensitivity. This solution is advantageous as it is computational efficient as proved by the performance indices along with a simplistic configuration due to a small number of setup parameters.

The second objective was achieved by the introduction of an improved cost-effective approach to optimal tuning of fuzzy controllers expressed as a four-step design method. This has beneficial effects in various servo systems and mechatronics applications.

The third objective was accomplished as a sustainable solution for the development of TSK PI-FCs with reduced sensitivity. This objective was supported by a sensitivity analysis with respect to the parametric variations of the controlled process.

Future research will approach other optimization problems, and their application to optimal control of complex applications.

ACKNOWLEDGMENT

This work was supported by grants from the Romanian Ministry of Research and Innovation, CNCS – UEFISCDI, project numbers PN-III-P1-1.1-PD2016-0683 and PN-III-P1-1.1-PD2016-0331, within PNCDI III, and the NSERC of Canada.

REFERENCES

- [1] R.-E. Precup, P. Angelov, B. S. J. Costa, and M. Sayed-Mouchaweh, "An overview on fault diagnosis and nature-inspired optimal control of industrial process applications," *Comput. Ind.*, vol. 74, pp. 75–94, Dec. 2015.
- [2] L.-K. Wang and H.-K. Lam, "Local stabilization for continuous-time takagi-sugeno fuzzy systems with time delay," *IEEE Trans. Fuzzy Syst.*, vol. 26, no. 1, pp. 379 – 385, Feb. 2018.
- [3] P. H. S. Coutinho, J. Lauber, M. Bernal, and R. M. Palhares, "Efficient LMI conditions for enhanced stabilization of discrete-time T-S models via delayed nonquadratic Lyapunov functions," *IEEE Trans. Fuzzy Syst.*, vol. 27, no. 9, pp. 1833–1843, Sep. 2019.
- [4] D. Leite, C. Aguiar, D. Pereira, G. Souza, and I. Škrjanc, "Nonlinear fuzzy state-space modeling and lmi fuzzy control of overhead cranes," in *Proc. 2019 IEEE International Conference on Fuzzy Systems*, New Orleans, LA, USA, 2019, pp. 1–6.
- [5] B. Zeren, M. Deveci, S. Coupland, R. John, and E. Özcan, "A study on the interpretability of a fuzzy system to control an inverted pendulum," in *Proc. 2019 IEEE International Conference on Fuzzy Systems*, New Orleans, LA, USA, 2019, pp. 1–6.
- [6] I. E. Herrera, A. Mandow, and A. García-Cerezo, "Using particle swarm optimization for fuzzy antecedent parameter identification in active suspension control," in *Proc. 2018 26th Mediterranean Conference on Control and Autom.*, Zadar, Croatia, 2018, pp. 1–9.
- [7] W. Zou, C. Li, and P. Chen, "An inter type-2 FCR algorithm based T-S fuzzy model for short-term wind power interval prediction," *IEEE Trans. Ind. Informat.*, vol. 15, pp. 4934–4943, Sep. 2019.
- [8] P. K. Ray, S. R. Paital, A. Mohanty, Y. S. E. Foo, A. Krishnan, H. B. Gooi, and G. A. J. Amarasingha, "A hybrid firefly-swarm optimized fractional order interval type-2 fuzzy PID-PSS for transient stability improvement," *IEEE Trans. Ind. Appl.*, vol. 55, no. 6, pp. 6486–6498, Nov.–Dec. 2019.
- [9] D. K. Lal, A. K. Barisal, and M. Tripathy, "GWO algorithm based fuzzy PID Controller for AGC of multi-area power system with TCPS," *Proc. Comput. Sci.*, vol. 92, pp. 99–105, Jan. 2016.
- [10] R.-E. Precup, R.-C. David, E. M. Petriu, A.-I. Szedlak-Stinean, and C.-A. Bojan-Dragos, "Grey wolf optimizer-based approach to the tuning of PI-fuzzy controllers with a reduced process parametric sensitivity," *IFAC-PapersOnLine*, vol. 49, no. 5, pp. 55–60, Jun. 2016.
- [11] R.-E. Precup, R.-C. David, and E. M. Petriu, "Grey wolf optimizer algorithm-based tuning of fuzzy control systems with reduced parametric sensitivity," *IEEE Trans. Ind. Electron.*, vol. 64, no. 1, pp. 527–534, Jan. 2017.
- [12] R.-C. Roman, R.-E. Precup, and R.-C. David, "Second order intelligent proportional-integral fuzzy control of twin rotor aerodynamic systems," *Proc. Comput. Sci.*, vol. 139, pp. 372–380, Oct. 2018.
- [13] R.-E. Precup, E.-I. Voisan, E. M. Petriu, M. L. Tomescu, R.-C. David, A.-I. Szedlak-Stinean, and R.-C. Roman, "Grey wolf optimizer-based approaches to path planning and fuzzy logic-based tracking control for mobile robots," *Int. J. Comput. Commun. Control*, vol. 15, no. 3, 3844, pp. 1–17, Jun. 2020.
- [14] S. Mirjalili and A. Lewis, "The whale optimization algorithm," *Adv. Eng. Softw.*, vol. 95, pp. 51–67, May 2016.
- [15] R. Sivalingam, S. Chinnamuthu, and S. S. Dash, "A modified whale optimization algorithm-based adaptive fuzzy logic PID controller for load frequency control of autonomous power generation systems," *Automatika*, vol. 58, no. 4, pp. 410–421, Dec. 2017.
- [16] P. R. Sahu, P. K. Hota, and S. Panda, "Modified whale optimization algorithm for coordinated design of fuzzy lead-lag structure-based SSSC controller and power system stabilizer," *Int. Trans. Electr. Energy Syst.*, vol. 29, no. 4, paper e2797, Apr. 2019.
- [17] M. Azizi, R. G. Ejlali, S. A. Mousavi Ghasemi, and S. Talatahari, "Upgraded whale optimization algorithm for fuzzy logic based vibration control of nonlinear steel structure," *Eng. Struct.*, vol. 192, pp. 53–70, Aug. 2019.
- [18] R.-C. David, R.-E. Precup, E. M. Petriu, M.-B. Radac, and S. Preitl, "Gravitational search algorithm-based design of fuzzy control systems with a reduced parametric sensitivity," *Inf. Sci.*, vol. 247, pp. 154–173, Oct. 2013.
- [19] S. Preitl and R.-E. Precup, "An extension of tuning relations after symmetrical optimum method for PI and PID controllers," *Automatica*, vol. 35, no. 10, pp. 1731–1736, Oct. 1999.
- [20] R.-E. Precup, R.-C. David, E. M. Petriu, S. Preitl, and M.-B. Radac, "Novel adaptive charged system search algorithm for optimal tuning of fuzzy controllers," *Expert Syst. Appl.*, vol. 41, no. 4, pp. 1168–1175, Mar. 2014.
- [21] S. Galichet and L. Fouloy, "Fuzzy controllers: synthesis and equivalences," *IEEE Trans. Fuzzy Syst.*, vol. 3, no. 2, pp. 140–148, May 1995.
- [22] R.-E. Precup and R.-C. David, *Nature-Inspired Optimization Algorithms for Fuzzy Controlled Servo Systems*. Oxford, UK: Butterworth-Heinemann, Elsevier, 2019.
- [23] R. Alcalá, J. Casillas, O. Cordón, A. González, and F. Herrera, "A genetic rule weighting and selection process for fuzzy control of heating, ventilating and air conditioning systems," *Eng. Appl. Artif. Intell.*, vol. 18, no. 3, pp. 279–296, Apr. 2005.
- [24] R.-E. Precup, M.-L. Tomescu, and C.-A. Dragos, "Stabilization of Rössler chaotic dynamical system using fuzzy logic control algorithm," *Int. J. Gen. Syst.*, vol. 43, no. 5, pp. 413–433, Jul. 2014.
- [25] S. Blažič, I. Škrjanc, and D. Matko, "A robust fuzzy adaptive law for evolving control systems," *Evolv. Syst.*, vol. 5, no. 1, pp. 3–10, Mar. 2014.
- [26] I. Dzitac, F. G. Filip, and M.-J. Manolescu, "Fuzzy logic is not fuzzy: World-renowned computer scientist Lotfi A. Zadeh," *Int. J. Comput. Communic. Control*, vol. 12, pp. 748–789, Dec. 2017.
- [27] L.-K. Wang and H.-K. Lam, "New stability criterion for continuous-time Takagi-Sugeno fuzzy systems with time-varying delay," *IEEE Trans. Cybern.*, vol. 49, no. 4, pp. 1551–1556, Apr. 2019.
- [28] Y. Jarraya, S. Bouaziz, H. Hagras, and A. M. Alimi, "A multi-agent architecture for the design of hierarchical interval type-2 beta fuzzy system," *IEEE Trans. Fuzzy Syst.*, vol. 27, no. 6, pp. 1174–1188, Jun. 2019.
- [29] I. H. Dridi, E.-B. Alaia, P. Borne, and H. Bouchriha, "Optimization of m-MDPPTW using the continuous and discrete PSO," *Stud. Informat. Control*, vol. 28, no. 3, pp. 289–298, Sep. 2019.
- [30] E. Osaba, J. Del Ser, D. Camacho, M. N. Bilbao, and X. S. Yang, "Community detection in networks using bio-inspired optimization: Latest developments, new results and perspectives with a selection of recent meta-heuristics," *Appl. Soft Comput.*, vol. 87, Feb. 2020.
- [31] Modular Servo System, User's Manual. Krakow: Inteco Ltd., 2007.